THE JOURNAL OF BIOLOGICAL CHEMISTRY
Vol. 278, No. 21, Issue of May 23, pp. 19220–19229, 2003
Printed in U.S.A.

The Shank Family of Postsynaptic Density Proteins Interacts with and Promotes Synaptic Accumulation of the βPIX Guanine Nucleotide Exchange Factor for Rac1 and Cdc42*

Received for publication, January 30, 2003, and in revised form, March 5, 2003
Published, JBC Papers in Press, March 7, 2003, DOI 10.1074/jbc.M301052200

Eunhye Park‡, Moonseok Na‡, Jeonghoon Choi‡, Seho Kim‡, Jae-Ran Lee‡, Jiyoung Yoon‡, Dongeun Park§, Morgan Sheng¶‖, and Eunjoon Kim‡**

From the ‡Department of Biological Sciences, Korea Advanced Institute of Science and Technology, Daejeon 305-701, Korea, the §School of Biological Sciences, Seoul National University, Seoul 151-742, Korea, and the ¶Picower Center for Learning and Memory, RIKEN-MIT Neuroscience Research Center and Howard Hughes Medical Institute, Massachusetts Institute of Technology, Cambridge, Massachusetts 02139

The Shank/ProSAP family of multidomain proteins is known to play an important role in organizing synaptic multiprotein complexes. Here we report a novel interaction between Shank and βPIX, a guanine nucleotide exchange factor for the Rac1 and Cdc42 small GTPases. This interaction is mediated by the PDZ domain of Shank and the C-terminal leucine zipper domain and the PDZ domain-binding motif at the extreme C terminus of βPIX. Shank colocalizes with βPIX at excitatory synaptic sites in cultured neurons. In brain, Shank forms a complex with βPIX and βPIX-associated signaling molecules including p21-associated kinase (PAK), an effector kinase of Rac1/Cdc42. Importantly, overexpression of Shank in cultured neurons promotes synaptic accumulation of βPIX and PAK. Considering the involvement of Rac1 and PAK in spine dynamics, these results suggest that Shank recruits βPIX and PAK to spines for the regulation of postsynaptic structure.

Dendritic spines are actin-rich morphological specializations in neurons that mediate most excitatory synaptic transmission (1–3). The postsynaptic density (PSD)[1] is a microscopic structure within dendritic spines that is associated with the postsynaptic membrane and contains a variety of scaffolding and signaling proteins (4, 5).

The Shank/ProSAP/SSTRIP family of multidomain proteins (Shank1, Shank2, and Shank3) plays important roles in organizing the PSD (6, 7). Shank is a relatively large protein (~200 kDa) and contains various protein interaction domains including, from the N terminus, ankyrin repeats, an SH3 domain, a PDZ domain, a long (>1000 aa residues) proline-rich region and a SAM domain. The ankyrin repeats interact with α-fodrin, an actin-regulating protein, and Sharpin, a protein implicated in Shank multimerization (8, 9). The Shank PDZ domain interacts with the GKAP/SAPAP family of synaptic scaffold proteins and various membrane proteins including the calcium-independent receptor for latrotoxin, somatostatin receptors, and metabotropic glutamate receptors (10–16). The long proline-rich region of Shank associates with IRSp53 (an insulin receptor tyrosine kinase substrate protein), Homer (an immediate early gene product that binds the group I metabotropic receptors and inositol 1,4,5-trisphosphate receptors), dynamin (a GTPase that regulates endocytosis), and cortactin (a regulator of the cortical actin cytoskeleton) (16–20). The C-terminal SAM domain mediates multimerization of Shank proteins (10). There are several splice variants of Shank with alternative translational start and stop codons, suggesting that the Shank protein interactions are regulated by alternative splicing (11, 12, 21, 22).

Functionally, Shank is involved in the morphogenesis of dendritic spines (3, 23). Overexpression of Shank proteins promotes the maturation of spines in cultured neurons (24). The enhanced spine maturation by Shank requires the interaction of Shank with Homer, a protein that binds to metabotropic glutamate receptors and inositol 1,4,5-trisphosphate receptors (16). In addition, expression of dominant-negative Shank constructs decreases spine density, suggesting that Shank is involved in spine formation or maintenance.

PIX/Cool is a family (αPIX and βPIX) of guanine nucleotide exchange factors for the Rac1 and Cdc42 small GTPases (25–27). PIX binds p21-activated kinase (PAK), a family of Rac/Cdc42-activated serine/threonine kinases (28), and promotes functional coupling of Rac1/Cdc42 and PAK (25). PIX also interacts with GIT/Cat/PKL/p95-APP, a family of multidomain signaling integrators with GTPase-activating protein activity for ADP ribosylation factor small GTPases, and regulates the dynamics of focal adhesion complexes (29). The function of PIX in neurons was suggested recently (30) by a genetic study on dPIX, a Drosophila homolog of PIX (31). Deletion of the *dpix* gene leads to defects in the structure of the neuromuscular junction and decreased synaptic levels of proteins including PAK, the PDZ domain-containing protein Dlg, and the glutamate receptor subunit GluRIIA (30). This suggests that PIX is an important organizer at the neuromuscular junction, but it remains unknown whether PIX plays a role in central synapses and, if so, how PIX regulates synaptic organization.

Here we report a novel interaction of Shank with βPIX and show that Shank promotes the synaptic localization of βPIX

* This work was supported in part by grants from the Korean Ministry of Science and Technology, the Korea Science and Engineering Foundation, and the Korea Research Foundation (to E. K.) and by National Research Laboratory Program M1-0203-00-0072 (to D. P.). The costs of publication of this article were defrayed in part by the payment of page charges. This article must therefore be hereby marked "*advertisement*" in accordance with 18 U.S.C. Section 1734 solely to indicate this fact.

‖ Investigator of the Howard Hughes Medical Institute.

** To whom correspondence should be addressed. Tel.: 42-869-2633; Fax: 42-869-2610; E-mail: kime@mail.kaist.ac.kr.

[1] The abbreviations used are: PSD, postsynaptic density; SH3, Src homology 3; SAM, sterile alpha motif; aa, amino acid(s); PAK, p21-associated kinase; EGFP, enhanced green fluorescent protein; HA, hemagglutinin; PH, pleckstrin homology; DH, Dbl homology; LZ, leucine zipper; GST, glutathione *S*-transferase; HEK, human embryonic kidney; MAP, mitogen-activated protein; DIV, days *in vitro*; GBD, GIT-binding domain.

and βPIX-associated PAK. In light of the fact that Rac/Cdc42 and PAK regulate the actin cytoskeleton (28) and that dendritic spines are actin-rich structures (2), our results suggest that Shank recruits βPIX and βPIX-associated proteins to spines and regulates postsynaptic structure.

EXPERIMENTAL PROCEDURES

Yeast Two-hybrid Assay—Yeast two-hybrid assay was performed using the L40 yeast strain as described previously (32). Full-length (aa 1–646) βPIX were amplified by PCR from mouse βPIX-a splice variant (27) and subcloned into the *Eco*RI-*Sal*I site of pBHA (a vector containing LexA DNA-binding domain). Small cDNA fragments of βPIX (aa 640–646 wild-type and point mutants) were generated by annealing oligonucleotides and subcloning them into the *Eco*RI-*Bam*HI site of pBHA. The following PDZ domains were subcloned into pGAD10 (a prey vector; Clontech): Shank2 PDZ (aa 30–137; *Bam*HI), Shank3 PDZ (aa 121–328; *Bam*HI-*Eco*RI), SAP97 PDZ1–2 (aa 224–404; *Bam*HI-*Eco*RI), GRIP2 PDZ1 (aa 41–136; *Bam*HI-*Eco*RI), GRIP2 PDZ2 (aa 148–245; *Bam*HI-*Eco*RI), and GRIP2 PDZ3 (aa 247–339; *Bam*HI-*Eco*RI). The other pGAD10 PDZ constructs have been described previously (32–34).

Antibodies—Polyclonal βPIX antibodies were generated by immunizing rabbits (1254) and guinea pigs (1257) with H6-βPIX (aa 294–646) as immunogen. Specific βPIX antibodies were affinity-purified after immobilizing the protein to a polyvinylidene difluoride membrane. The following antibodies have been described: EGFP (1167) (35), PSD-95 (SM55) (35), Shank (3856, pan-Shank) (10), Shank (1123, pan-Shank) (9), and GIT1 (du139) (36). The following antibodies were obtained from commercial sources: HA rabbit polyclonal (Santa Cruz Biotechnology), FLAG M2 monoclonal (Sigma), synaptophysin SVP38 (Sigma), MAP2 (Sigma), phospho-neurofilament H N52 (Sigma), PAK N-20 (Santa Cruz Biotechnology), vinculin hVIN-1 (Sigma), and p130Cas (Transduction Laboratories).

Expression Constructs—To generate various EGFP-tagged βPIX constructs, the following regions of βPIX were PCR amplified and subcloned into pEGFP-C1 (Clontech) using the indicated enzyme sites: full-length (aa 1–646; *Sal*I-*Kpn*I), SH3 (aa 1–70; *Eco*RI-*Bam*HI), DH (aa 89–286; *Eco*RI-*Kpn*I), PH (aa 280–417; *Eco*RI-*Bam*HI), PXXP (aa 396–502; *Eco*RI-*Bam*HI), GBD (aa 486–566; *Eco*RI-*Bam*HI), LZ (aa 575–642; *Eco*RI-*Bam*HI), ΔSH3 (aa 61–646; *Eco*RI-*Kpn*I), ΔDH (aa 1–646 Δ100–279; *Sal*I-*Kpn*I-*Bam*HI), ΔPH (aa 1–646 Δ287–400; *Sal*I-*Kpn*I-*Kpn*I), ΔPXXP (aa 1–646 Δ407–494; *Sal*I-*Kpn*I-*Kpn*I), ΔGBD (aa 1–646 Δ496–555; *Sal*I-*Kpn*I-*Kpn*I), ΔLZ (aa 1–646 Δ587–639; *Eco*RI-*Kpn*I-*Kpn*I), ΔETNL (aa 1–642; *Eco*RI-*Kpn*I), and Δ(LZ-ETNL) (aa 1–586; *Eco*RI-*Kpn*I). EGFP-tagged full-length αPIX (aa 1–728) was subcloned into the *Eco*RI site of pEFGP-C1. The last seven aa of βPIX (aa 640–646) and GKAP (aa 660–666) were generated by annealing oligonucleotides and subcloning them into the *Kpn*I-*Bam*HI site of pEGFP-C1. The following constructs have been described: FLAG-tagged full-length GIT1 (36), HA-tagged full-length Shank2 and Shank3 (21), and HA-tagged full-length and deletion variants of Shank1B (24).

GST Pull Down Assay—For pull down, the last seven aa of βPIX (wild-type and L646A mutant) were generated by annealing oligonucleotides and subcloning them into the *Bam*HI-*Eco*RI site of pGEX4T-1. The PDZ domain of Shank1 (aa 584–690) was subcloned into the *Bam*HI site of pGEX4T-1. For pull down, HEK293T cells were transfected with various βPIX constructs, GIT1, GKAP last seven aa, and Shank2. Two days after transfection, HEK293T cells were harvested and extracted by incubating with phosphate-buffered saline containing 1% Triton X-100 (for cells transfected with various βPIX and GIT1) or with radioimmune precipitation assay buffer (pH 7.5, 50 mM Tris-HCl, 150 mM NaCl, 1% Nonidet P-40, 0.5% sodium deoxycholate, and 0.1% SDS; for cells transfected with GKAP last seven aa and Shank2) at 4 °C for 30 min. After centrifugation, the supernatant was incubated with 5 μg of GST fusion proteins, or GST alone, for 30 min at room temperature, followed by precipitation with glutathione-Sepharose 4B resin. The precipitates were analyzed by immunoblotting with antibodies against HA (0.4 μg/ml), EGFP (1167, 1:1000), and FLAG (1 μg/ml).

Preparation of PSD and Subcellular Fractions—Subcellular fractionation of rat brain was performed as described previously (37). Adult (~6 weeks) rat brains were homogenized in ice-cold homogenization buffer (0.32 M sucrose, 4 mM HEPES, pH 7.3) supplemented with protease inhibitors. After centrifuging the homogenates twice at 900 and 1000 × *g* for 10 min, the supernatant was centrifuged at 12000 × *g* for 15 min. The supernatant was saved as the cytosolic fraction (S2). The pellet was resuspended in homogenization buffer and centrifuged at 13000 × *g* for 15 min to obtain the crude synaptosomal fraction (pellet, P2). PSD fractions were purified as described previously (38).

Coimmunoprecipitation Assay in Heterologous Cells and in Rat Brain—Transfected HEK293T cells were extracted with binding buffer (phosphate-buffered saline containing 1% Triton X-100 or radioimmune precipitation assay buffer) and incubated with HA-agarose (Sigma) or antibodies against EGFP (1167; 4 μg/ml) at 4 °C for 90 min, followed by precipitation with protein A-Sepharose (Amersham Biosciences). For *in vivo* coimmunoprecipitation, the crude synaptosomal fraction of adult rat brain was solubilized with DOC buffer (50 mM Tris-HCl, 1% sodium deoxycholate, pH 9.0), dialyzed against binding/dialysis buffer (50 mM Tris-HCl, 0.1% Triton X-100, pH 7.4), and centrifuged. The supernatant was incubated with βPIX (1254; 7 μg/ml) antibody, Shank (3856; 10 μg/ml) antibody, or rabbit IgG (10 μg/ml; negative control) for 2 h and then with protein A-Sepharose for 2 h. The precipitates were analyzed by immunoblotting with antibodies against EGFP (1167; 1:1000), HA (0.4 μg/ml), βPIX (1254; 0.2 μg/ml or 1257; 1 μg/ml), Shank (3856; 1:2000), GIT1 (du139; 1:2000), PAK (1 μg/ml), vinculin (1:1000), and p130Cas (1:1000).

Immunohistochemistry on Rat Brain Sections—Adult rats were perfused with 4% paraformaldehyde, and brain sections (50 μm) were cut using a vibratome. Brain sections were permeabilized by incubation in phosphate-buffered saline containing 50% ethanol at room temperature for 30 min. For immunofluorescence staining, brain sections were incubated with βPIX (1254; 1 μg/ml) antibodies overnight at room temperature, followed by Cy3-conjugated secondary antibodies (Jackson ImmunoResearch Laboratories) for 2 h at room temperature. Images were captured using a LSM510 confocal laser scanning microscope (Zeiss).

Primary Neuron Culture, Transfection, and Immunocytochemistry—Cultured hippocampal neurons were prepared from embryonic (E18) rat brain as described (39). Disassociated neurons were placed in neurobasal medium supplemented with B27, 0.5 mM L-glutamine, 12.5 μM glutamate, and penicillin-streptomycin (Invitrogen) for 3 h and grown in fresh medium without glutamate. Low density cultures were used for colocalization studies. At 21 days *in vitro* (DIV), hippocampal neurons were fixed and permeabilized with precooled methanol at −20 °C for 15 min and incubated with primary antibodies against βPIX (1254; 1 μg/ml), Shank (1123; 1:150), synaptophysin (1:200), MAP2 (1:500), neurofilament-H (1:500), and PAK (10 μg/ml), followed by Cy3- or fluorescein isothiocyanate-conjugated secondary antibodies. Neurons were transfected at DIV 19 using a mammalian transfection kit (Invitrogen) and stained at DIV 21 using the same method used for colocalization experiments.

Image Acquisition and Analysis—Images were analyzed blind using MetaMorph image analysis software (Universal Imaging). The parameter settings were kept constant for all scans. Transfected neurons were chosen randomly for quantitation from immunostained coverslips from two to three independent experiments. Synaptic areas were defined as discrete Shank-positive regions. For each neuron studied, the synaptic targeting of βPIX was determined by measuring the average fluorescence intensity of βPIX in 10 individual synaptic areas per neuron. Statistical significance was determined by Student's *t* test. *N* numbers refer to the number of neurons quantified.

RESULTS

Interaction between Shank and βPIX in Vitro—We reported recently (40) that βPIX is enriched in the PSD and associates with the GIT-liprin-α-GRIP complex that is involved in the regulation of synaptic targeting of alpha-amino-3-hydroxy-5-methyl-4-isoxazolepropionic acid glutamate receptors. We noticed that the C terminus of βPIX ends with Asp-Glu-Thr-Asn-Leu (DETNL), a sequence that fits to the class I PDZ-binding consensus (41) and closely mimics that of GKAP/SAPAP (QTRL), a family of proteins that interact with Shank (42–44). When tested for binding to various PDZ domains in a yeast two-hybrid assay, the C terminus of βPIX interacted with the PDZ domains from the Shank family proteins (Shank1, Shank2, and Shank3) but not with those from other proteins including PSD-95, SAP97, S-SCAM, GRIP1, and GRIP2/ABP (Fig. 1*A*). A point mutation of the βPIX C terminus in which the last aa, Leu-646, of βPIX was converted into Ala (DETN<u>A</u>) but not a conserved mutation (D<u>Q</u>TNL) eliminated the Shank-βPIX interaction (Fig. 1*B*). Intriguingly mutation of the Asp residue at the −4 position to Asn (<u>N</u>ETNL and <u>NQ</u>TNL) elim-

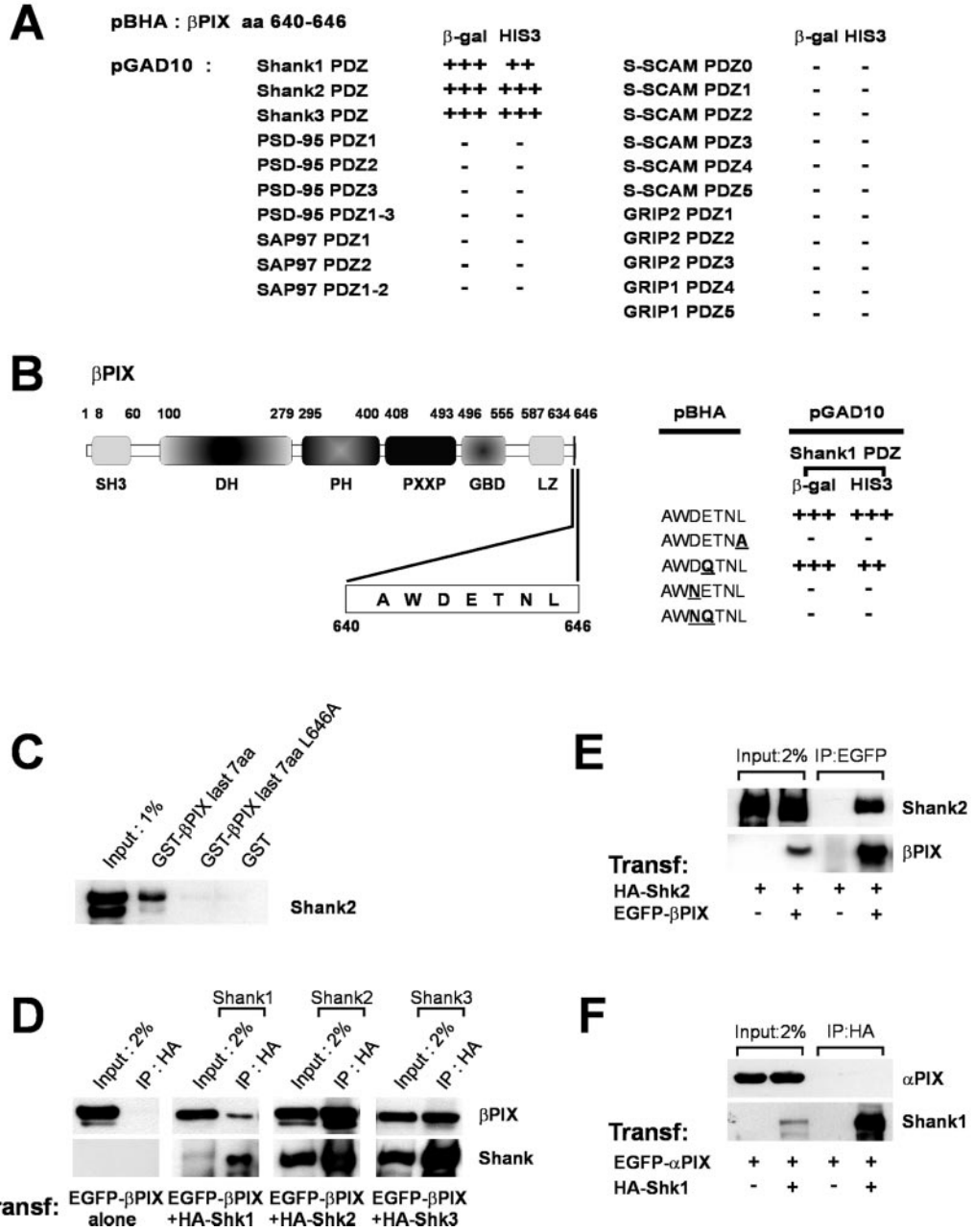

FIG. 1. **Characterization of the interaction between Shank and βPIX *in vitro*.** *A*, specific interaction of βPIX with Shank PDZ domains in the yeast two-hybrid assay. The last seven aa residues of βPIX in pBHA were tested for binding to PDZ domains from various PDZ-domain-containing proteins in pGAD10. HIS3 activity was as follows: +++, >60%; ++, 30–60%; +, 10–30%; −, no significant growth. β-Galactosidase was as follows: +++, <45 min; ++, 45–90 min; +, 90–240 min; −, no significant β-galactosidase activity. *B*, interaction of the C terminus of βPIX with Shank. Variants of the βPIX C terminus (wild-type and point mutants of the backbone of the last seven aa residues) in pBHA were tested against Shank1 PDZ in pGAD10 in a yeast two-hybrid assay. *PXXP*, proline-rich region. *Small numbers* refer to aa residues at the boundaries of domains. The mutated residues are *underlined* in *bold*. *C*, pull down of Shank by GST fusion proteins of βPIX (last seven residues, wild-type, and point mutant). Lysates of HEK293T cells transfected with HA-Shank2 were pulled down by indicated βPIX GST fusion proteins and characterized by immunoblotting with HA antibodies. *D* and *E*, coimmunoprecipitation between Shank and βPIX in heterologous cells. HEK293T cell lysates transfected with full-length HA-Shanks (*Shk*) + EGFP-βPIX, EGFP-βPIX alone, or HA-Shank2 alone were immunoprecipitated with HA or EGFP antibodies and characterized by immunoblotting with HA and EGFP antibodies. *Transf*, transfection; *IP*, immunoprecipitation. *F*, absence of detectable interaction between Shank and αPIX in coimmunoprecipitation assay.

inated the Shank-βPIX interaction (Fig. 1*B*), suggesting that the residues upstream of the known PDZ-binding consensus sites (in general the last three residues) are also important for PDZ recognition in the Shank-βPIX interaction.

In GST pull down assay, a GST fusion protein containing the last seven residues of βPIX (GST-βPIX last seven aa) but not GST alone pulled down Shank2 expressed in HEK293T cells (Fig. 1*C*). However, a GST-βPIX last seven aa mutant in which the last residue Leu was changed into Ala (GST-βPIX last seven aa L646A) did not pull down Shank2. These results are consistent with the yeast two-hybrid results and indicate that the Shank-βPIX interaction is mediated by the canonical PDZ-peptide interaction.

In HEK293T cell lysates doubly transfected with HA-tagged Shanks (HA-Shank1, HA-Shank2, or HA-Shank3) and EGFP-tagged βPIX (EGFP-βPIX), HA antibodies immunoprecipitated HA-Shanks and coprecipitated βPIX (Fig. 1*D*). HA antibodies did not bring down singly expressed βPIX. Conversely, incuba-

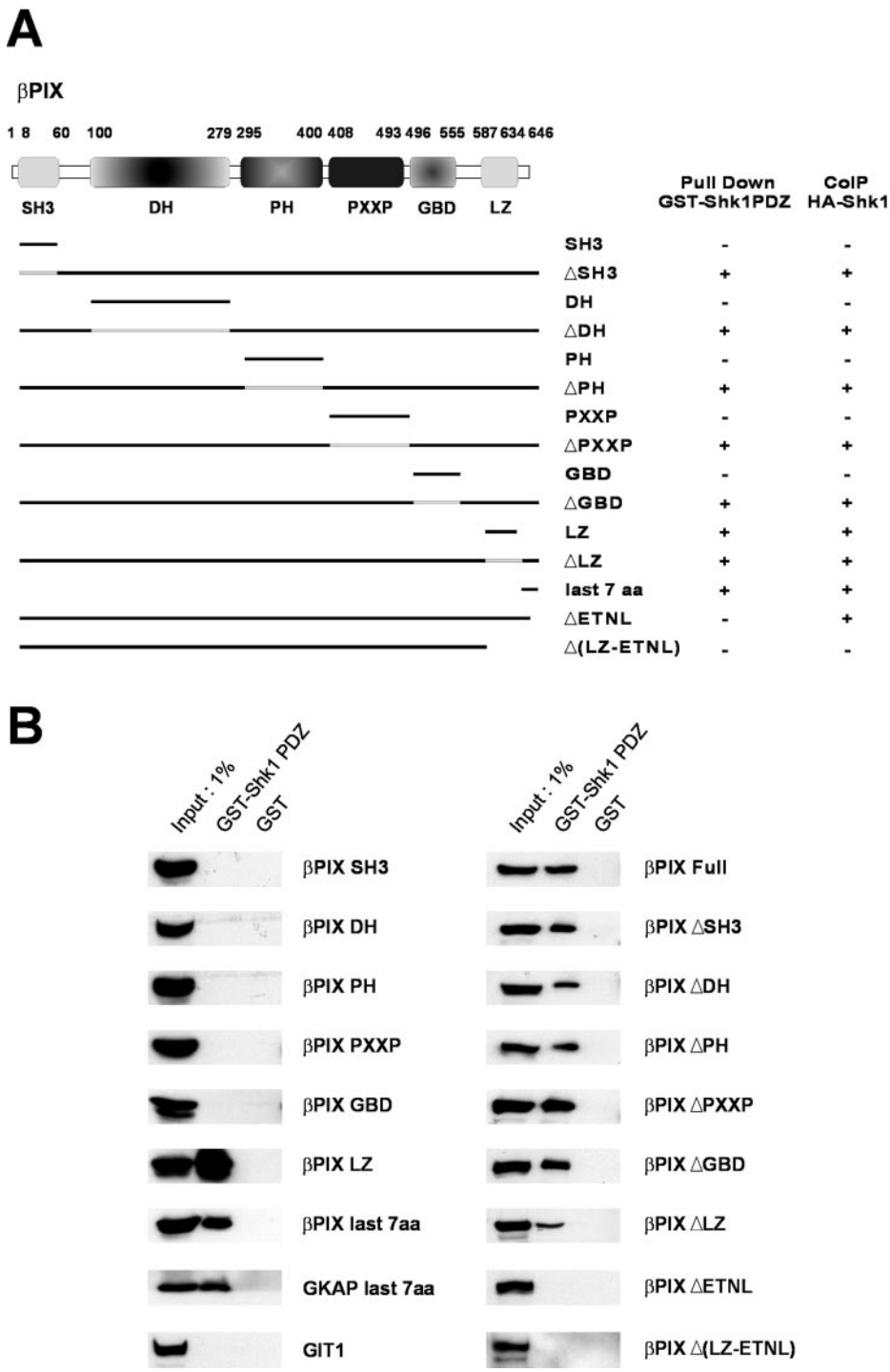

FIG. 2. **The LZ domain and the C-terminal PDZ-binding motif of βPIX mediate the interaction with Shank in a pull down assay.** *A*, diagram depicting deletion variants of βPIX and summary of their interaction with Shank in pull down (Fig. 2) and coimmunoprecipitation (Fig. 3) assays. *CoIP*, coimmunoprecipitation. *B*, pull down of βPIX (individual domains and deletion variants) by Shank1 PDZ. Lysates of HEK293T cells transfected with indicated EGFP-βPIX variants were pulled down by GST-Shank1 PDZ, and the precipitates were characterized by immunoblotting with EGFP antibodies.

tion of the cell lysates doubly transfected with HA-Shank2 + EGFP-βPIX with EGFP antibodies brought down βPIX and coprecipitated HA-Shank (Fig. 1*E*). These results indicate that full-length Shank and βPIX form a coimmunoprecipitable complex in heterologous cells.

The PIX family contains two members, αPIX and βPIX, that share similar domain structure (25). Like βPIX, αPIX contains an LZ domain that shares 75% aa sequence identity with the βPIX LZ domain, although αPIX does not have a PDZ-binding motif at its C terminus. However, αPIX did not coimmunoprecipitate with Shank1 (Fig. 1*F*), suggesting that Shank specifically interacts with βPIX but not with αPIX.

The LZ Domain and the C-terminal PDZ-binding Motif of βPIX Mediate the Interaction with the PDZ Domain of Shank—Although the results mentioned above clearly suggest that the C-terminal PDZ-binding motif of βPIX interacts with the PDZ domain of Shank, it is possible that other regions of Shank and βPIX may mediate the interaction. We first tested this possibility by pulling down various deletion variants of βPIX (depicted in Fig. 2*A*) with the GST fusion protein containing the PDZ domain of Shank1 (GST-Shank1 PDZ) (Fig. 2*B*). GST-Shank1 PDZ pulled down the last seven aa residues of βPIX (EGFP-βPIX last seven aa), as expected. Intriguingly, GST-Shank1 PDZ also pulled down EGFP-βPIX containing the LZ domain with a strong coiled-coil property (EGFP-βPIX LZ), suggesting that the LZ domain of βPIX also binds to the PDZ domain of Shank. In contrast, none of the other domains of βPIX (SH3, DH, PH, PXXP, and GBD) was pulled down by

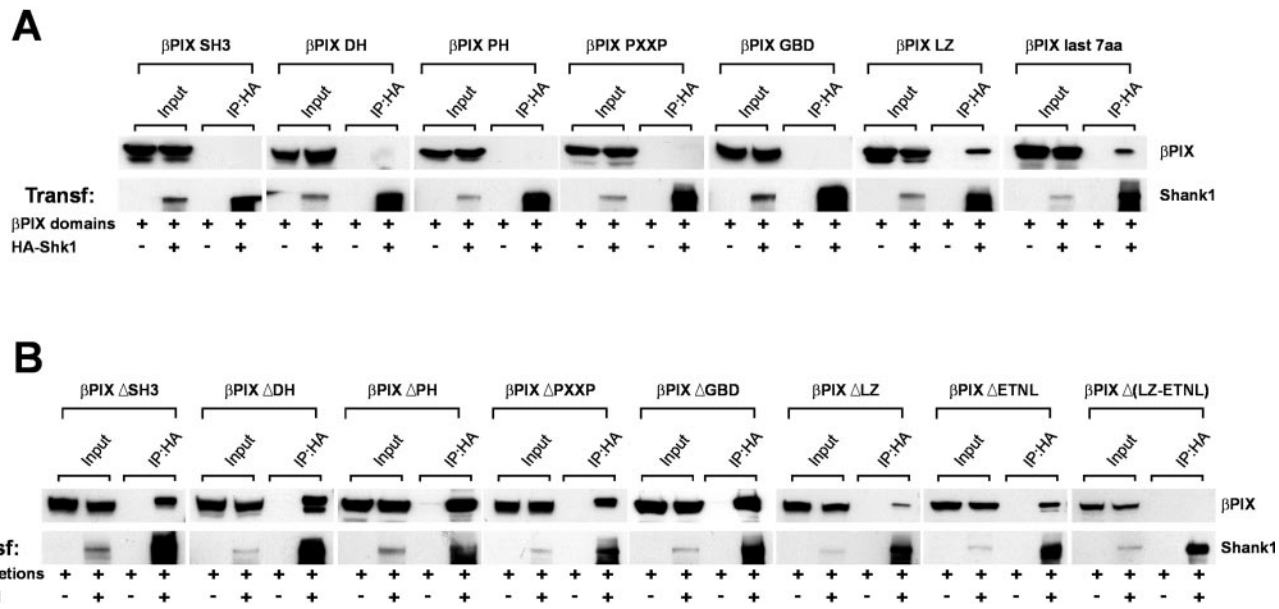

FIG. 3. **The LZ domain and the C-terminal PDZ-binding motif of βPIX mediate the interaction with Shank in a coimmunoprecipitation assay.** Lysates of HEK293T cells doubly transfected with HA-Shank1 + EGFP-βPIX individual domains (*A*), HA-Shank1 + EGFP-βPIX deletions variants (*B*) or singly transfected with EGFP-βPIX variants were immunoprecipitated by HA-agarose and characterized by immunoblotting with HA and EGFP antibodies. Input, 2%.

GST-Shank1 PDZ. Consistently, βPIX deletions lacking the LZ domain (EGFP-βPIX ΔLZ) and the last four residues (EGFP-βPIX ΔETNL) showed a significantly reduced and undetectable pull down, respectively, by GST-Shank1 PDZ. As expected, EGFP-βPIX lacking the region from the LZ domain to the C terminus (EGFP-βPIX Δ(LZ-ETNL)) was not pulled down by the Shank PDZ. In contrast, deletion of the other domains of βPIX (ΔSH3, ΔDH, ΔPH, ΔPXXP, and ΔGBD) did not affect the pull down of βPIX by the Shank PDZ. These results indicate that the LZ domain and the C-terminal PDZ-binding motif of βPIX mediate its interaction with Shank.

In coimmunoprecipitation assays, EGFP-βPIX LZ or EGFP-βPIX last seven aa but not other domains of βPIX formed a complex with HA-Shank1 full-length in transiently transfected HEK293T cells (Fig. 3*A*). Consistently, EGFP-βPIX ΔLZ and EGFP-βPIX ΔETNL showed reduced coimmunoprecipitation with Shank (Fig. 3*B*), and EGFP-βPIX Δ(LZ-ETNL) completely lost its Shank binding. In contrast, deletion of the other domains in βPIX (ΔSH3, ΔDH, ΔPH, ΔPXXP, and ΔGBD) did not affect the coimmunoprecipitation of βPIX with Shank. The small but significant coimmunoprecipitation observed in EGFP-βPIX ΔETNL (Fig. 3*B*) contrasts with the complete loss of its interaction with the Shank PDZ in the pull down assay (Fig. 2*B*). This could be because of the fact that the Shank constructs used in the two assays were different; the PDZ domain and the full-length were used in the pull down and coimmunoprecipitation assays, respectively. Indeed, EGFP-βPIX ΔETNL failed to coimmunoprecipitate with HA-Shank1 PDZ (data not shown), although further details remain to be determined. Taken together, these results, summarized in Fig. 2*A*, further confirm that the LZ domain and the C-terminal PDZ-binding motif of βPIX mediate its interaction with Shank.

Conversely, in HEK293T cells cotransfected with EGFP-βPIX full-length and HA-Shank1B deletion variants (depicted in Fig. 4*A*), all of the HA-Shank deletion variants containing the PDZ domain coimmunoprecipitated with βPIX (Fig. 4*B*). In contrast, Shank deletions lacking the PDZ domain did not show any detectable coimmunoprecipitation with βPIX. These results, summarized in Fig. 4*A*, suggest that the PDZ domain of Shank is the major determinant of βPIX binding.

Spatiotemporal Expression of βPIX and Its Association with Shank in Rat Brain—To study βPIX *in vivo*, in particular its spatiotemporal expression and the association with Shank, we generated polyclonal antibodies against βPIX (rabbit 1254 and guinea pig 1257) using a H6 fusion protein containing the second half (aa 294–646) of βPIX as immunogen. The 1254 βPIX antibody specifically recognized βPIX but not αPIX in immunoblot analysis (Fig. 5*A*). Similar results were obtained for the 1257 βPIX antibody (data not shown). In rat brain, the βPIX (1254) antibody recognized four major bands (66–105 kDa; see Fig. 5*B*), which may represent splice variants of βPIX (45, 46). In support of this, one of the brain βPIX bands matched the size of the βPIX-a splice variant expressed in heterologous cells (Fig. 5*B*).

Expression of βPIX proteins was detected in various brain regions including the cortex, cerebellum, and hippocampus (Fig. 5*C*). During the postnatal development of rat brain, expression levels of βPIX reached a peak around postnatal day 7 and then gradually decreased to adult levels (Fig. 5*D*). This contrasts with the steady increase in expression levels of PSD-95 and Shank during the first 3 weeks of postnatal development (Fig. 5*D*). In contrast to the reported enrichment of βPIX and βPIX-binding GIT1 in the PSD (40), PAK, another βPIX-binding protein, was not enriched in the PSD although a significant portion of PAK was detected in the crude synaptosomal fraction as was βPIX (Fig. 5*E*), suggesting that PAK is not a core component of the PSD.

We next determined whether Shank and βPIX form a complex in brain. Incubation of extracts of the crude synaptosomal fraction of adult rat brain with βPIX antibodies brought down βPIX and coprecipitated Shank and βPIX-associated GIT1 and PAK (Fig. 5*F*). Irrelevant proteins such as vinculin and p130Cas were not coimmunoprecipitated with βPIX. Conversely, Shank antibodies pulled down Shank and coprecipitated βPIX, GIT1, and PAK but not vinculin and p130Cas (Fig. 5*G*). These results suggest that Shank forms a complex with βPIX and βPIX-associated proteins in brain.

Shank and βPIX Colocalize at Synaptic Sites in Cultured Neurons—Shank proteins are mainly localized to synaptic sites

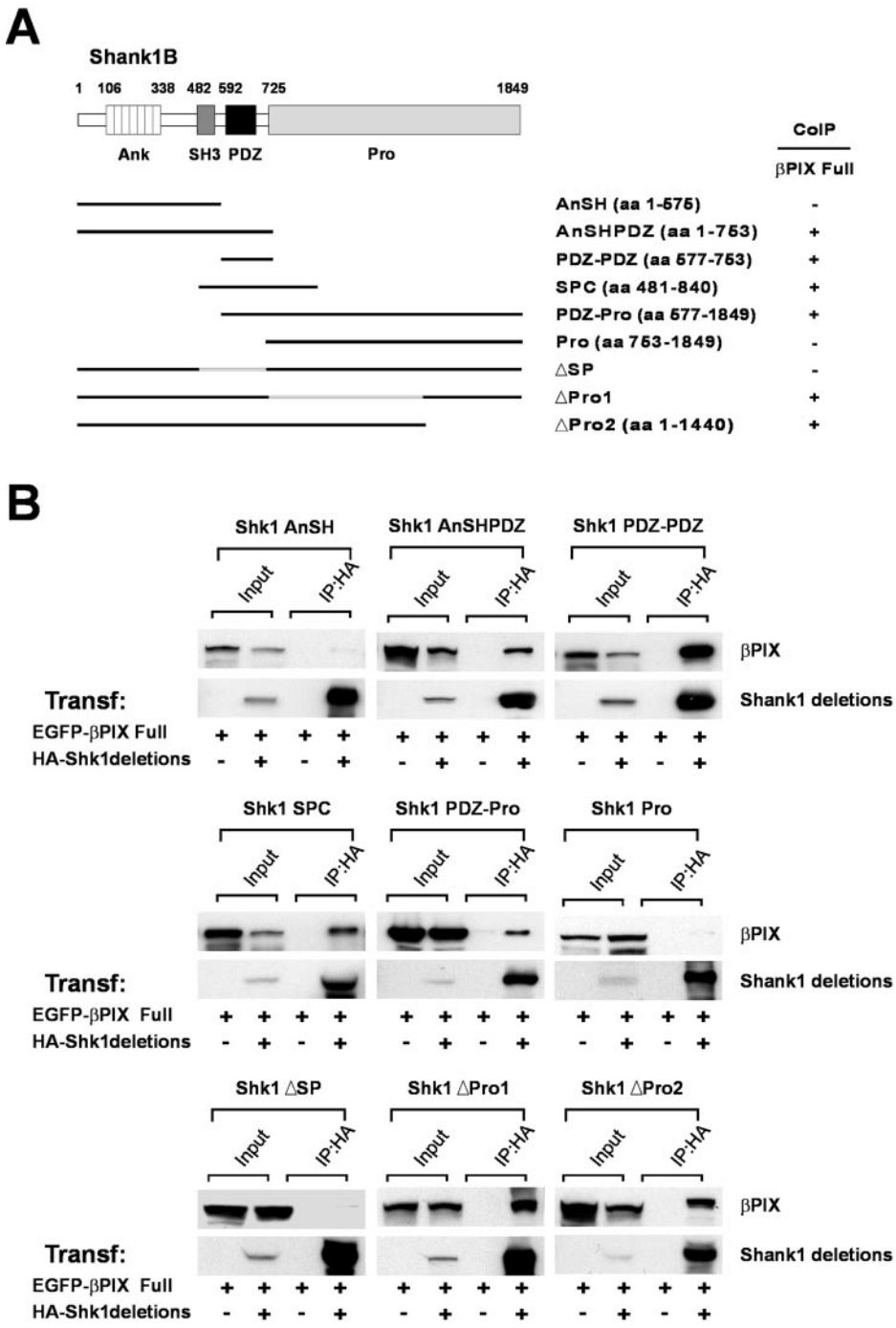

FIG. 4. **The PDZ domain of Shank mediates the interaction with βPIX.** *A*, diagram depicting deletion variants of Shank1B, a splice variant of Shank1 lacking the C-terminal SAM domain (24), and summary of their interaction with βPIX in coimmunoprecipitation assays. *Ank*, ankyrin repeats; *PDZ*, PSD-95/Dlg/ZO-1 domain; *Pro*, proline-rich region. *PDZ-PDZ* indicates a tandem construct. *B*, coimmunoprecipitation of βPIX with deletion variants of Shank1B. Lysates of HEK293T cells transfected with EGFP-βPIX full-length + HA-Shank1B deletion variants, or EGFP-βPIX full-length alone, were immunoprecipitated with HA-agarose and characterized by immunoblotting with HA and EGFP antibodies. Input, 2%.

in cultured neurons (10, 11). However, little is known about the subcellular distribution pattern of βPIX. Using the βPIX (1254) antibody, we determined the subcellular distribution of βPIX in cultured hippocampal neurons (DIV 21) (Fig. 6). Immunofluorescence signals of βPIX colocalized with both MAP2-positive dendrites and MAP2-negative axons (*arrow*; see Fig. 6*A*). Consistently, βPIX colocalized with neurofilament-H-positive axons (Fig. 6*B*, *arrow*), suggesting that βPIX distributes to both dendrites and axons. At higher magnifications, βPIX immunoreactivity was mainly detected in punctate structures (Fig. 6*C1*). Some of the punctate βPIX-positive structures colocalized with synaptophysin, a marker for the presynaptic nerve terminal, but a significant portion of βPIX structures did not (Fig. 6*C*), suggesting that βPIX proteins are widely distributed to both synaptic and non-synaptic sites. Some βPIX signals colocalized with Shank (Fig. 6*D*), suggesting that βPIX is localized to excitatory synaptic sites.

Distribution of βPIX in Brain Regions—In rat brain slices, immunofluorescence signals of βPIX were widely detected in various regions of rat brain including the cortex (Fig. 7*A*), hippocampus (Fig. 7*B*), and cerebellum (Fig. 7*C*). At higher magnifications, strong βPIX signals were observed in hippocampal pyramidal neurons (Fig. 7, *D* and *E*, examples from CA1 and CA3 regions of hippocampus, respectively) and cerebellar Purkinje cells (Fig. 7*F*). Preincubation of βPIX antibodies with immunogen eliminated the signal (data not shown). Double immunofluorescence staining for βPIX and glial fibrillary acidic protein, a marker for glial cells, showed no colocalization between the two proteins at least in cortex and hippocampus (data not shown), suggesting that βPIX is mainly

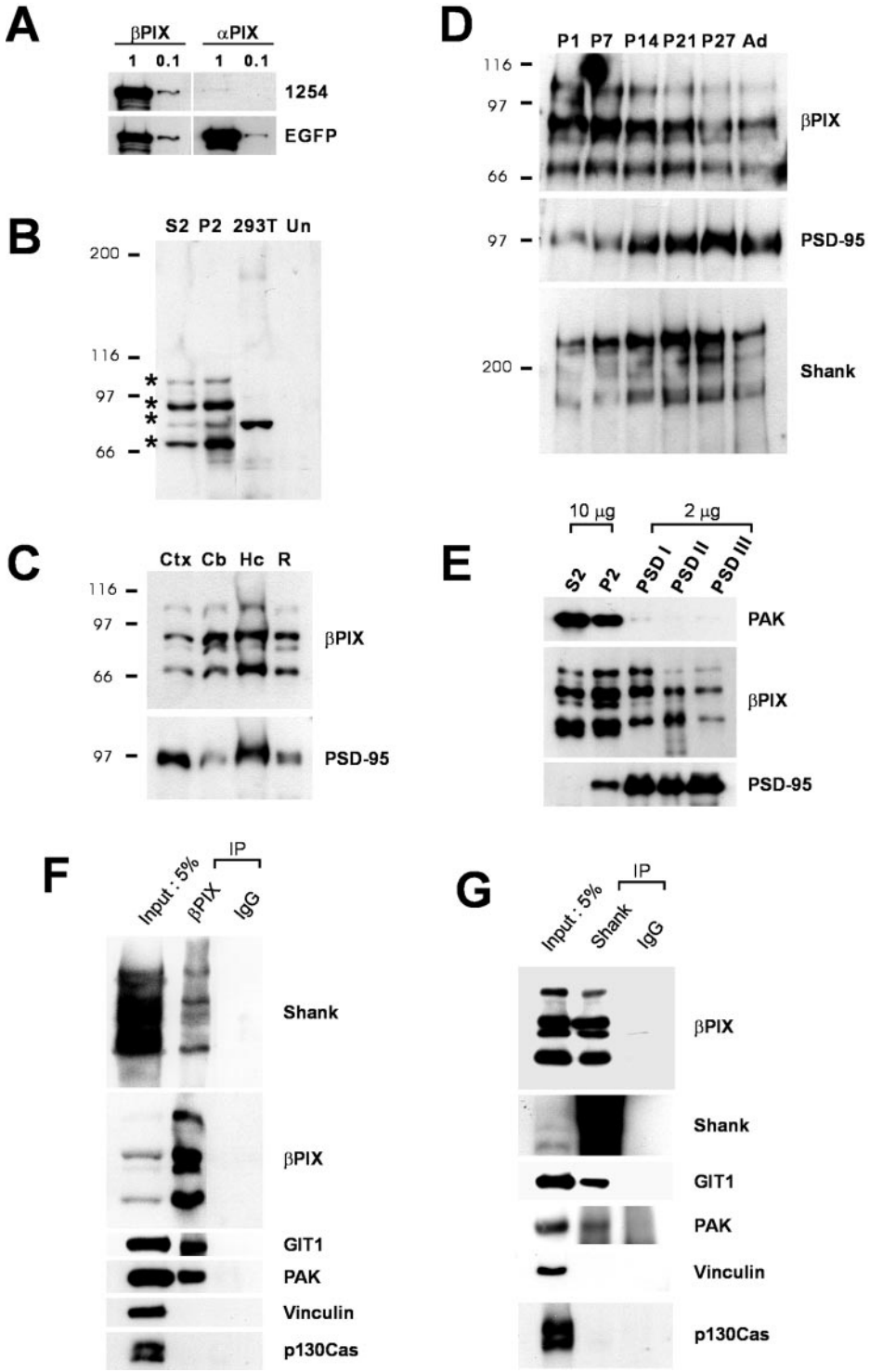

FIG. 5. **Spatiotemporal expression pattern of βPIX and its association with Shank in rat brain.** *A*, specific recognition of βPIX by the 1254 βPIX antibody. HEK293T cells transfected with EGFP-αPIX or EGFP-βPIX were characterized by immunoblotting with βPIX (1254) and EGFP (for normalization) antibodies. The numbers (*1* and *0.1*) indicate relative amounts of proteins loaded. *B*, βPIX proteins expressed in brain. The crude synaptosomal (*P2*) and cytosolic (*S2*) fractions of adult rat brain were immunoblotted with βPIX (1254) antibodies. The *asterisks* indicate βPIX bands expressed in brain, one of which matches the size of the βPIX-a splice variant expressed in HEK293T (*293T*) cells. *Un*, untransfected HEK293T cells. *C*, expression of βPIX in various brain regions. Total homogenates of adult rat brain regions were immunoblotted with βPIX (1254) and PSD-95 (Sm55) antibodies. *Ctx*, cortex; *Cb*, cerebellum; *Hc*, hippocampus; *R*, other regions of the brain. *D*, expression of βPIX during postnatal brain development. Total homogenates of rat brain at various stages of postnatal development were immunoblotted with βPIX (1254), PSD-95, and Shank (3856) antibodies. *P1*, postnatal day 1; *Ad*, adult (6 weeks). *E*, lack of PSD enrichment in PAK. PSD fractions extracted with Triton X-100 once (*PSD I*), twice (*PSD II*), or with Triton X-100 and a strong detergent Sarcosyl (*PSD III*) were immunoblotted with PAK, βPIX (1254), and PSD-95 antibodies. *F* and *G*, coimmunoprecipitation of Shank with βPIX and βPIX-associated proteins in brain. Detergent lysates of the crude synaptosomal fraction of adult rat brain were immunoprecipitated with βPIX (1254), Shank (3856), or rabbit IgG (*IgG*) and characterized by immunoblotting with the indicated antibodies.

expressed in neurons. Taken together, these results suggest that βPIX is widely expressed in brain regions.

Overexpression of Shank in Cultured Neurons Promotes Synaptic Accumulation of βPIX and PAK—The majority of Shank proteins distribute to synaptic sites (10, 11), whereas a significant portion of βPIX staining is detected at extrasynaptic sites (Fig. 6, *C* and *D*). Biochemically, Shank proteins are mainly detected in the crude synaptosomal fraction of rat brain (9), whereas βPIX distributes to both synaptosomal and cytosolic fractions (Fig. 5*E*) (40). These results suggest the hypothesis that Shank may recruit βPIX to spines. To this end, we tested the effect of Shank overexpression on the subcellular localization of endogenous βPIX in cultured neurons (Fig. 8). Overexpression of Shank1B in cultured hippocampal neurons markedly increased the colocalization of endogenous βPIX with Shank (Fig. 8*A*), in contrast to the partial synaptic localization of βPIX in untransfected neurons (Fig. 6, C and *D*). Quantitative analysis indicated that the immunofluorescence staining intensity of βPIX at synapses (as defined by the average fluorescence intensity of βPIX in synaptic area) was significantly increased in Shank-overexpressing neurons (181.2 ± 25.7, $n = 30$ cells; *, $p < 0.0001$; see Fig. 8*D*), compared with untransfected neurons (111.1 ± 41.6, $n = 30$; see Fig. 8*D*). These results, considering a previous report that overexpressed Shank proteins are mostly targeted to postsynaptic spines (24), suggest that Shank promotes accumulation of βPIX in dendritic spines. In addition, synaptic labeling of PAK

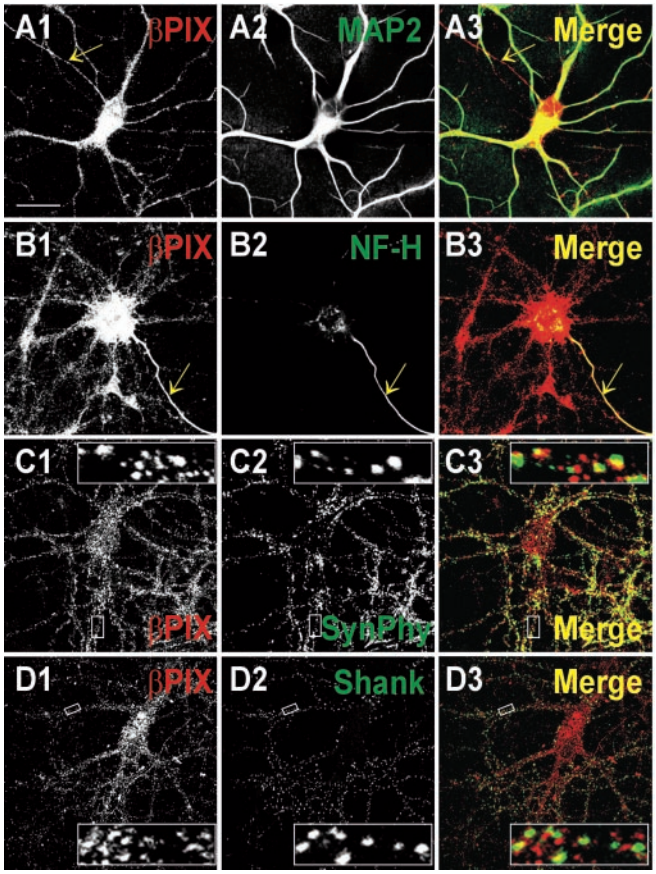

FIG. 6. **Subcellular localization of βPIX and its colocalization with Shank in cultured neurons.** Cultured hippocampal neurons (DIV 21) were stained by double immunofluorescence staining for βPIX (1254) (*red*) and MAP2, neurofilament-H (*NF-H*), synaptophysin (*Syn-Phy*), or Shank (1123) (*green*). *Arrows* in *A* and *B* indicate axons. Merged images of A1 + A2, B1 + B2, and C1 + C2 are shown in *A3*, *B3*, and *C3*, respectively. *Scale bar*, 30 μm.

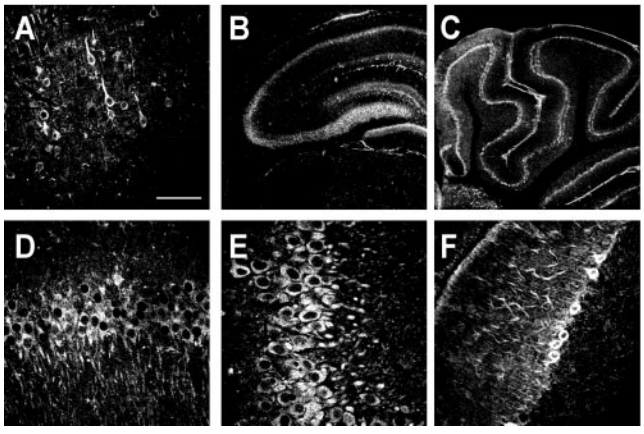

FIG. 7. **Distribution of βPIX in brain regions.** Adult rat brain slices were incubated with βPIX (1254) antibodies, followed by Cy3-conjugated secondary antibodies. *A*, cortex; *B*, hippocampus; *C*, cerebellum; *D*, CA1 region of hippocampus; *E*, CA3 region of hippocampus; *F*, cerebellum at a higher magnification. The *scale bar* was as follows: A, 100 μm; *B* and *C*, 400 μm; *D* and *E*, 50 μm; *F*, 100 μm.

was also significantly increased by Shank overexpression (190.3 ± 18.3, $n = 25$; *, $p < 0.0001$; see Fig. 8, *B* and *E*), relative to untransfected neurons (136.0 ± 28.7, $n = 25$; see Fig. 8, *C* and *E*). Taken together, these results suggest that Shank promotes recruitment of βPIX and PAK to spines.

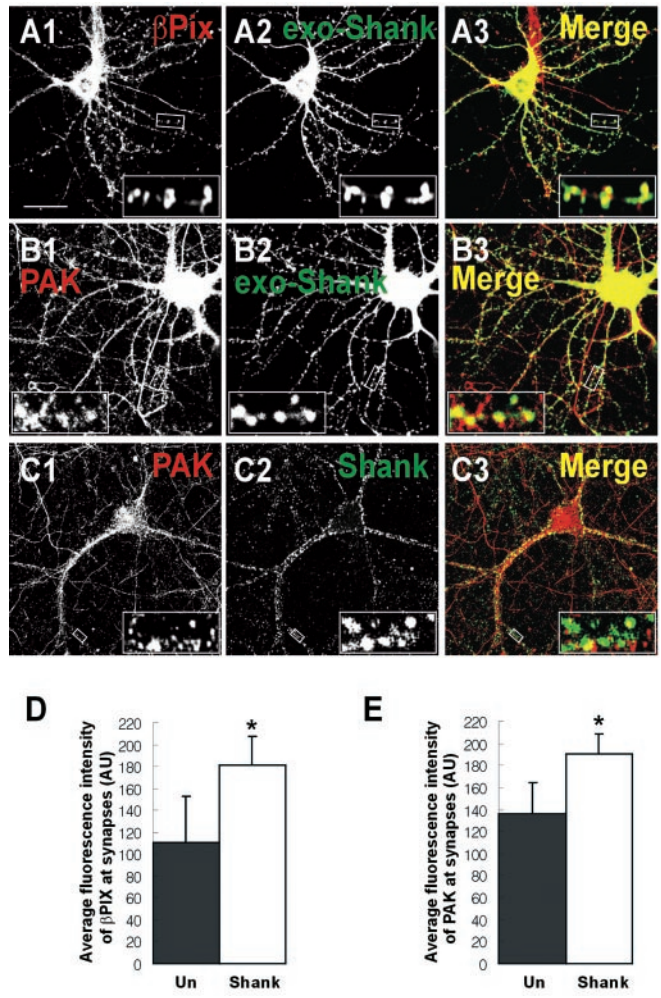

FIG. 8. **Overexpression of Shank in cultured neurons promotes accumulation of βPIX and PAK in dendritic spines.** *A* and *B*, cultured hippocampal neurons (DIV 19) were transfected with HA-Shank1B (*exo-Shank*), and changes in the subcellular distribution of endogenous βPIX and endogenous PAK were monitored by double immunofluorescence staining for βPIX (*A1*, *red*; 1254, rabbit polyclonal), PAK (*B1*, *red*; rabbit polyclonal), and Shank (*A2* and *B2*, *green*; 1123, guinea pig polyclonal) at DIV 21. Neurons expressing exogenous Shank could be easily identified by their higher immunofluorescence relative to neighboring untransfected neurons. *C*, limited colocalization of endogenous PAK and Shank. Cultured hippocampal neurons (DIV 21) were doubly labeled for PAK (*C1*, *red*) and Shank (*C2*, *green*). *Scale bar*, 30 μm. *D* and *E*, quantitation of changes in spine accumulation of βPIX (*D*) and PAK (*E*) induced by Shank overexpression. Immunofluorescence staining intensities of βPIX and PAK at synapses (as defined by the average fluorescence intensity of βPIX and PAK in synaptic area) in untransfected (*Un*) and transfected (*Shank*) neurons were compared. Histograms show mean ± S.D. *, $p < 0.0001$. *AU*, arbitrary unit.

DISCUSSION

A Novel Mode of Protein-Protein Interactions in the Shank PDZ Domain—Our results indicate that both the LZ domain and the C-terminal PDZ-binding motif of βPIX are involved in the interaction with the PDZ domain of Shank. We recently determined (47) the crystal structure of the Shank PDZ in a complex with a peptide mimicking the C-terminal PDZ-binding motif of GKAP/SAPAP.[2] The structure of the Shank PDZ-peptide complex indicates an association of the peptide with the peptide-binding groove, a well known region in the PDZ domain for peptide binding (41). Assuming that a similar binding mode also applies to the interaction between the Shank PDZ and the βPIX C terminus, the LZ domain of βPIX is likely to bind to a

[2] S. Park, E. Kim, and S. Eom, unpublished data.

region of the Shank PDZ outside the groove. The participation of "non-groove" surfaces of the PDZ domain in protein interactions is not uncommon. The PDZ7 of GRIP1 uses a novel hydrophobic surface distinct from the groove to interact with GRASP-1 (48), a neuronal Ras guanine nucleotide exchange factor (49). Similarly, a novel surface of the PDZ6 of GRIP1 outside the groove mediates self-dimerization (50). This mode of parallel binding, simultaneous binding of the LZ and the extreme C terminus to the PDZ, may ensure a stronger interaction between Shank and βPIX and/or provide additional sites for regulation of the interaction.

The LZ domain of βPIX is known to mediate homo- and heterodimerization (46, 51). It remains to be determined whether the dimerization affects the Shank-βPIX interaction or vice versa. However, if these two interactions occur independently, the Shank-βPIX interaction may function as a mechanism to bring additional βPIX and βPIX-binding proteins (PAK, Rac1/Cdc42, and GIT) into the vicinity of Shank. Alternatively, βPIX dimers may further stabilize Shank multimers that are known to be formed by the C-terminal SAM domain (10). This hypothesis is reminiscent of the proposed functions of Homer that, through self-multimerization, links Shank to inositol 1,4,5-trisphosphate receptors and metabotropic glutamate receptors (10, 16, 24).

Functions of the Interaction between Shank and βPIX—Overexpression of Shank in cultured neurons promotes synaptic accumulation of βPIX (Fig. 8, *A* and *D*), suggesting that Shank recruits βPIX to spines. This model is supported by the immunohistochemical and biochemical results that Shank mainly distributes to synaptic sites (9–11, 16, 22) whereas βPIX is partially synaptic (see Fig. 5*E* and Fig. 6, *C* and *D*) (40). This is also consistent with the hypothesis that Shank, through local translation of dendritic Shank mRNAs, may act as a scaffold recruiting various synaptic proteins to spines (6, 13).

In addition to βPIX, synaptic accumulation of PAK is also increased by Shank overexpression (Fig. 8, *B* and *E*). The enhanced synaptic accumulation of PAK appears to occur through its interaction with βPIX. In support of this, βPIX is enriched in the PSD (Fig. 5*E*) (40), whereas PAK is not enriched in the PSD although a significant fraction of it is present in the crude synaptosomal fraction (Fig. 5*E*). Critically, a *Drosophila* genetic study demonstrated that mutations in the *dpix* gene lead to a complete loss of synaptic localization of dPAK (30). These results are also consistent with the results from non-neuronal cells that βPIX binding is required for localization of PAK to focal complexes (25).

How might Shank promote synaptic accumulation of βPIX? It may occur through the direct or indirect interaction between Shank and βPIX, which are not mutually exclusive. Previously, Sala *et al.* (24) have shown that the Shank-induced synaptic accumulation of Homer is eliminated by mutations that disrupt the Shank-Homer interaction. However, we could not take a similar approach, because the PDZ domain of Shank, the region to which βPIX binds, has been shown to be critical for synaptic targeting of Shank (24), making it impossible to distinguish between direct and indirect mechanisms. Nevertheless, it has been shown in non-neuronal cells that the LZ domain of βPIX is critical for targeting of βPIX to the cell periphery and inducing membrane ruffles and microvillus-like structures (46, 51). These results and our finding that the βPIX LZ binds to the Shank PDZ support the first hypothesis of direct recruitment, although further details remain to be elucidated.

Neuronal Functions of βPIX—We demonstrated that the expression levels of βPIX reaches a peak around postnatal day 7 and then decreases gradually to adult levels (Fig. 5*D*). Because dendritic spines are in general poorly developed during early postnatal stages (1–2 weeks), the high levels of βPIX around the first week suggest that βPIX may have roles in developing neurons. βPIX activates Rac1 and Cdc42 (25), small GTPases known to regulate various aspects of neuronal morphogenesis including neurite initiation, growth, guidance, branching, polarity, and synapse formation (52). Thus βPIX expressed at early developmental stages may have a role associated with the Rac/Cdc42-dependent regulation of neuronal morphogenesis.

We observed steady, although reduced, levels of βPIX expression in the later stages of postnatal development (Fig. 5*D*), suggesting that βPIX also has functions in mature neurons. In mature neurons, βPIX is localized to excitatory synaptic sites (Fig. 6*D*), enriched in the PSD (Fig. 5*E*) (40), and redistributed, along with PAK, to synaptic sites by Shank (Fig. 8), suggesting that βPIX may regulate functions associated with dendritic spines. In dendritic spines, βPIX may induce local activation of Rac1/Cdc42 and PAK, molecules known to regulate spine morphogenesis. Constitutively active Rac1 leads to the development of supernumerary spines of very small sizes in cerebellar Purkinje neurons of transgenic mice (53) and generation of filopodia- and lamellipodia-like structures in neurons of rat hippocampal and cortical slices (54, 55). In contrast, dominant-negative Rac1 leads to a progressive elimination of dendritic spines in hippocampal slices (55). Consistently, Kalirin-7, a brain-specific guanine nucleotide exchange factor for Rac1 enriched in the PSD (56), interacts with various PDZ-containing proteins including PSD-95 (57) and, by upstream stimulation of Eph receptors, increases the number and size of spine-like structures in transfected neurons in a Rac1- and PAK-dependent manner (57–59). PAK is known to regulate the actin cytoskeleton (28), a major determinant of the shape, stability, and plasticity of dendritic spines (2, 60–62). In *Drosophila*, dPAK is a key mediator of the dPIX-dependent regulation of postsynaptic structure and protein targeting (30). Taken together, our data, along with previous results, suggest that Shank may regulate spine dynamics through synaptic accumulation of βPIX and local activation of the Rac1-PAK signaling pathway. It has been reported (24) that overexpression of Shank in cultured neurons promotes spine maturation while not affecting spine density and that overexpression of dominant-negative constructs of Shank reduces spine density. Considering the association of Shank with βPIX, a possible interpretation of these results is that overexpressed dominant-negative Shank proteins may inhibit synaptic targeting of endogenous Shank that is required for spine recruitment of βPIX and formation/maintenance of dendritic spines.

In conclusion, we have demonstrated that Shank associates with βPIX and recruits βPIX and PAK to synaptic sites. These molecular mechanisms may contribute to Shank-dependent organization of the PSD and to the regulation of dendritic spine dynamics. We are currently investigating the functions of βPIX and βPIX-associated proteins in the morphogenesis of dendritic spines.

Acknowledgment—We are grateful to Dr. Carlo Sala at CNR Institute of Neuroscience for the gift of Shank deletion constructs.

REFERENCES

1. Harris, K. M., and Kater, S. B. (1994) *Annu. Rev. Neurosci.* **17,** 341–371
2. Matus, A. (2000) *Science* **290,** 754–758
3. Hering, H., and Sheng, M. (2001) *Nat. Rev. Neurosci.* **2,** 880–888
4. Kennedy, M. B. (2000) *Science* **290,** 750–754
5. Sheng, M., and Kim, M. J. (2002) *Science* **298,** 776–780
6. Sheng, M., and Kim, E. (2000) *J. Cell Sci.* **113,** 1851–1856
7. Boeckers, T. M., Bockmann, J., Kreutz, M. R., and Gundelfinger, E. D. (2002) *J. Neurochem.* **81,** 903–910
8. Bockers, T. M., Mameza, M. G., Kreutz, M. R., Bockmann, J., Weise, C., Buck, F., Richter, D., Gundelfinger, E. D., and Kreienkamp, H. J. (2001) *J. Biol. Chem.* **276,** 40104–40112
9. Lim, S., Sala, C., Yoon, J., Park, S., Kuroda, S., Sheng, M., and Kim, E. (2001)

Mol. Cell. Neurosci. **17,** 385–397
10. Naisbitt, S., Kim, E., Tu, J. C., Xiao, B., Sala, C., Valtschanoff, J., Weinberg, R. J., Worley, P. F., and Sheng, M. (1999) *Neuron* **23,** 569–582
11. Yao, I., Hata, Y., Hirao, K., Deguchi, M., Ide, N., Takeuchi, M., and Takai, Y. (1999) *J. Biol. Chem.* **274,** 27463–27466
12. Zitzer, H., Honck, H. H., Bachner, D., Richter, D., and Kreienkamp, H. J. (1999) *J. Biol. Chem.* **274,** 32997–33001
13. Zitzer, H., Richter, D., and Kreienkamp, H. J. (1999) *J. Biol. Chem.* **274,** 18153–18156
14. Kreienkamp, H. J., Zitzer, H., Gundelfinger, E. D., Richter, D., and Bockers, T. M. (2000) *J. Biol. Chem.* **275,** 32387–32390
15. Tobaben, S., Sudhof, T. C., and Stahl, B. (2000) *J. Biol. Chem.* **275,** 36204–36210
16. Tu, J. C., Xiao, B., Naisbitt, S., Yuan, J. P., Petralia, R. S., Brakeman, P., Doan, A., Aakalu, V. K., Lanahan, A. A., Sheng, M., and Worley, P. F. (1999) *Neuron* **23,** 583–592
17. Okamoto, P. M., Gamby, C., Wells, D., Fallon, J., and Vallee, R. B. (2001) *J. Biol. Chem.* **276,** 48458–48465
18. Du, Y., Weed, S. A., Xiong, W. C., Marshall, T. D., and Parsons, J. T. (1998) *Mol. Cell. Biol.* **18,** 5838–5851
19. Bockmann, J., Kreutz, M. R., Gundelfinger, E. D., and Bockers, T. M. (2002) *J. Neurochem.* **83,** 1013–1017
20. Soltau, M., Richter, D., and Kreienkamp, H. J. (2002) *Mol. Cell. Neurosci.* **21,** 575–583
21. Lim, S., Naisbitt, S., Yoon, J., Hwang, J. I., Suh, P. G., Sheng, M., and Kim, E. (1999) *J. Biol. Chem.* **274,** 29510–29518
22. Boeckers, T. M., Kreutz, M. R., Winter, C., Zuschratter, W., Smalla, K. H., Sanmarti-Vila, L., Wex, H., Langnaese, K., Bockmann, J., Garner, C. C., and Gundelfinger, E. D. (1999) *J. Neurosci.* **19,** 6506–6518
23. Ehlers, M. D. (2002) *Trends Neurosci.* **25,** 64–67
24. Sala, C., Piech, V., Wilson, N. R., Passafaro, M., Liu, G., and Sheng, M. (2001) *Neuron* **31,** 115–130
25. Manser, E., Loo, T. H., Koh, C. G., Zhao, Z. S., Chen, X. Q., Tan, L., Tan, I., Leung, T., and Lim, L. (1998) *Mol. Cell* **1,** 183–192
26. Bagrodia, S., Taylor, S. J., Jordon, K. A., Van Aelst, L., and Cerione, R. A. (1998) *J. Biol. Chem.* **273,** 23633–23636
27. Oh, W. K., Yoo, J. C., Jo, D., Song, Y. H., Kim, M. G., and Park, D. (1997) *Biochem. Biophys. Res. Commun.* **235,** 794–798
28. Bagrodia, S., and Cerione, R. A. (1999) *Trends Cell Biol.* **9,** 350–355
29. Turner, C. E., West, K. A., and Brown, M. C. (2001) *Curr. Opin. Cell Biol.* **13,** 593–599
30. Parnas, D., Haghighi, A. P., Fetter, R. D., Kim, S. W., and Goodman, C. S. (2001) *Neuron* **32,** 415–424
31. Werner, L. A., and Manseau, L. J. (1997) *Gene* **187,** 107–114
32. Kim, E., Niethammer, M., Rothschild, A., Jan, Y. N., and Sheng, M. (1995) *Nature* **378,** 85–88
33. Mok, H., Shin, H., Kim, S., Lee, J. R., Yoon, J., and Kim, E. (2002) *J. Neurosci.* **22,** 5253–5258
34. Wyszynski, M., Kim, E., Dunah, A. W., Passafaro, M., Valtschanoff, J. G., Serra-Pages, C., Streuli, M., Weinberg, R. J., and Sheng, M. (2002) *Neuron* **34,** 39–52
35. Choi, J., Ko, J., Park, E., Lee, J. R., Yoon, J., Lim, S., and Kim, E. (2002) *J. Biol. Chem.* **277,** 12359–12363
36. Premont, R. T., Claing, A., Vitale, N., Freeman, J. L., Pitcher, J. A., Patton, W. A., Moss, J., Vaughan, M., and Lefkowitz, R. J. (1998) *Proc. Natl. Acad. Sci. U. S. A.* **95,** 14082–14087
37. Huttner, W. B., Schiebler, W., Greengard, P., and De Camilli, P. (1983) *J. Cell Biol.* **96,** 1374–1388
38. Cho, K. O., Hunt, C. A., and Kennedy, M. B. (1992) *Neuron* **9,** 929–942
39. Goslin, K., and Banker, G. (1991) in *Culturing Nerve Cells* (Banker, G., and Goslin, K., eds), The MIT Press, Cambridge, MA
40. Ko, J., Kim, S., Valtschanoff, J. G., Shin, H., Lee, J. R., Sheng, M., Premont, R. T., Weinberg, R. J., and Kim, E. (2003) *J. Neurosci.* **23,** 1667–1677
41. Sheng, M., and Sala, C. (2001) *Annu. Rev. Neurosci.* **24,** 1–29
42. Kim, E., Naisbitt, S., Hsueh, Y. P., Rao, A., Rothschild, A., Craig, A. M., and Sheng, M. (1997) *J. Cell Biol.* **136,** 669–678
43. Takeuchi, M., Hata, Y., Hirao, K., Toyoda, A., Irie, M., and Takai, Y. (1997) *J. Biol. Chem.* **272,** 11943–11951
44. Satoh, K., Yanai, H., Senda, T., Kohu, K., Nakamura, T., Okumura, N., Matsumine, A., Kobayashi, S., Toyoshima, K., and Akiyama, T. (1997) *Genes Cells* **2,** 415–424
45. Kim, S., Kim, T., Lee, D., Park, S. H., Kim, H., and Park, D. (2000) *Biochem. Biophys. Res. Commun.* **272,** 721–725
46. Koh, C. G., Manser, E., Zhao, Z. S., Ng, C. P., and Lim, L. (2001) *J. Cell Sci.* **114,** 4239–4251
47. Park, S. H., Im, Y. J., Rho, S. H., Lee, J. H., Yang, S., Kim, E., and Eom, S. H. (2002) *Acta Crystallogr. Sect. D Biol. Crystallogr.* **58,** 1353–1355
48. Feng, W., Fan, J. S., Jiang, M., Shi, Y. W., and Zhang, M. (2002) *J. Biol. Chem.* **277,** 41140–41146
49. Ye, B., Liao, D., Zhang, X., Zhang, P., Dong, H., and Huganir, R. L. (2000) *Neuron* **26,** 603–617
50. Im, Y. J., Park, S. H., Rho, S. H., Lee, J. H., Kang, G. B., Sheng, M., Kim, E., and Eom, S. H. (2002) *J. Biol. Chem.* **278,** 8501–8507
51. Kim, S., Lee, S. H., and Park, D. (2001) *J. Biol. Chem.* **276,** 10581–10584
52. Luo, L. (2000) *Nat. Rev. Neurosci.* **1,** 173–180
53. Luo, L., Hensch, T. K., Ackerman, L., Barbel, S., Jan, L. Y., and Jan, Y. N. (1996) *Nature* **379,** 837–840
54. Tashiro, A., Minden, A., and Yuste, R. (2000) *Cereb. Cortex* **10,** 927–938
55. Nakayama, A. Y., Harms, M. B., and Luo, L. (2000) *J. Neurosci.* **20,** 5329–5338
56. Penzes, P., Johnson, R. C., Alam, M. R., Kambampati, V., Mains, R. E., and Eipper, B. A. (2000) *J. Biol. Chem.* **275,** 6395–6403
57. Penzes, P., Johnson, R. C., Sattler, R., Zhang, X., Huganir, R. L., Kambampati, V., Mains, R. E., and Eipper, B. A. (2001) *Neuron* **29,** 229–242
58. Penzes, P., Beeser, A., Chernoff, J., Schiller, M. R., Eipper, B. A., Mains, R. E., and Huganir, R. L. (2003) *Neuron* **37,** 263–274
59. Penzes, P., Johnson, R. C., Kambampati, V., Mains, R. E., and Eipper, B. A. (2001) *J. Neurosci.* **21,** 8426–8434
60. Allison, D. W., Gelfand, V. I., Spector, I., and Craig, A. M. (1998) *J. Neurosci.* **18,** 2423–2436
61. Kim, C. H., and Lisman, J. E. (1999) *J. Neurosci.* **19,** 4314–4324
62. Krucker, T., Siggins, G. R., and Halpain, S. (2000) *Proc. Natl. Acad. Sci. U. S. A.* **97,** 6856–6861